Wide area tracking method for augmented reality supporting nuclear power plant maintenance work

ISHII Hirotake[1], YAN Weida[1], YANG Shou-feng[1], SHIMODA Hiroshi[1], and **IZUMI Masanori[2]**

1. Graduate School of Energy Science, Kyoto University, Kyoto 611-0011, Japan
2. Fugen Decommissioning Engineering Center, Japan Atomic Energy Agency, Tsuruga 914-8510, Japan

Abstract: A new fiducial marker for augmented reality was designed along with a method that recognizes the markers captured by a camera and calculates the relative position and orientation between the markers and the camera. These markers can be used at both long and short distances without increasing the number of markers pasted in the environment. Results of the experimental evaluation show that the new marker can be used in a larger area than legacy markers such as square markers and circular markers.
Keyword: tracking method; augmented reality; maintenance support; multi-range fiducial marker
CLC number: **Document code: A Article ID:** 1671-9433(2007)01-0000-00

1 Introduction

Augmented Reality (AR) is a technology that makes us feel that virtual objects and symbols actually exist in front of us by superimposing computer-generated images on our view. [1] For workers in nuclear power plants (NPPs), various supports can be accomplished by applying AR because it can show three-dimensional positions and orientations to workers more intuitively than legacy interfaces such as paper-based instruction documents. [2–4] For example, workers can be navigated safely and effectively if the direction in which they should walk is shown according to their current position and orientation (Navigation function). It can also show dangerous areas (Safety function) and working procedures (Instruction function) intuitively to the workers.

For applying AR to support NPP workers, a tracking method that measures the position and orientation of the workers in real time is indispensable. However, existing tracking methods such as Global Positioning System (GPS), magnetic sensors, ultrasonic sensors, and inertial sensors can not be used in NPPs: GPS can not be used inside buildings; magnetic sensors and ultrasonic sensors are not useful in complicated environments with many metal instruments; and inertial sensors' error increases over time. [1]

In this study, we specifically examine marker-based tracking methods [5–10], which calculate the relative position and orientation between a camera and markers using image processing and geometry calculation. Such methods present advantages: they can be used inside buildings, are unaffected by metal and loud noise, and remain accurate even over a long time. However, existing marker-based tracking methods are useful only under limited conditions. For example, square markers [5–7] are useful only for short distances between a camera and markers. On the other hand, line markers [8][9] and circular markers [10] are useful only at great distances. Therefore, both square markers and line/circular markers must be pasted in work areas when AR is used in NPPs, where workers are expected to move throughout a large area. However, it is difficult to paste many markers in NPPs because the interior of the NPP buildings is complicated, with insufficient space for pasting many markers.

For this study, therefore, we designed a new marker that is useful at both long and short distances and developed a method that recognizes the markers captured by a camera and calculates the relative position and orientation between the markers and the camera. Moreover, experimental evaluations were conducted to evaluate the newly designed markers' performance. The required performance of the tracking method used in NPPs varies according to the application (the purpose of the support). For this study,

Received date :

we aimed at developing a tracking method for which the position accuracy is about 20 cm (half a step of a human walking) and for which the orientation accuracy is about 20 deg (18 directions), which is expected to be sufficient for realizing the Navigation function, Safety function, and Instruction function, which support operation of large instruments such as pumps and motors in NPPs.

2 Proposal of a tracking method using multi-range markers

2.1 Design of multi-range markers

Figure 1 portrays a design example of the multi-range marker proposed for this study. This marker consists of one large circle located in the marker's center and four small circles in the marker's four corners. The centers of one large and four small circles are used as feature points of the marker. The feature points are recognized by image processing; they are used for the tracking calculation. To obtain a unique solution, four or more feature points on the camera image must be recognized simultaneously. [11]

The large circle has one black outer circle, one white center circle, and one middle circle, which consists of 10 black or white fans that represent a binary code by their color. The thickness of the outer circle, center circle and middle circle are 30%, 30% and 40% of the large circle's radius respectively.

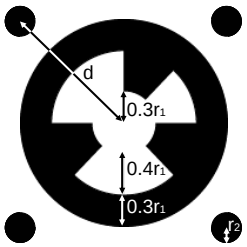

Fig. 1 Design example of multi-range marker.

For using this multi-range marker in NPPs, the markers are pasted on the surface of instruments that must be maintained and walls near the instruments. The three-dimensional positions of the markers must be measured in advance. The camera used for tracking is equipped on the worker's helmet or the backside of a portable computer or a PDA.

The workers refer to information provided by AR far from instruments and walls when they use the Navigation function or the Safety function. In this case, the distance between a camera and the markers is great. Thereby, the camera captures plural markers, but they are small on the image. When a marker on the image is small, it is easy to recognize the large circle, but it is difficult to recognize the small circles. Therefore, only one feature point is obtainable from one marker, but sufficient feature points for tracking are obtainable from plural markers. On the other hand, when workers use the Instruction function, the workers refer to information provided by AR near instruments and walls. In this case, the distance between a camera and markers becomes short. Therefore, a few markers can be captured, but they are large on the image. When a marker on the image is large, it is easy to recognize the small circles. Therefore, sufficient feature points for tracking are obtainable from one marker.

2.2 Algorithm to recognize multi-range markers

An algorithm to recognize multi-range markers is described in this section. For the following algorithm, it is assumed that the multi-range markers are printed out on white paper with printers and that the image obtained from a camera is in gray-scale format: each image pixel has a value of 0–255.

Step 1-1. Obtain an image from a camera and convert each pixel ($I(x, y)$) using Eqs. (1) and (2).

i) When $0 \le I(x, y) \le 127$, then

$$J(x, y) = \log_{10}(I(x, y) + 1) . \quad (1)$$

ii) When $128 \le I(x, y) \le 255$, then

$$J(x, y) = 4.243 - \log_{10}(266 - I(x, y)) . \quad (2)$$

Step 1-2. Apply a 3×3 Sobel edge detector to the image obtained in Step 1-1 and binarize the result with a threshold of 0.8.

Step 1-3. Label the binarized image by collecting the connected pixels and assigning a unique label. Eliminate candidates with area less than 10 or greater than 100000.

Step 1-4. Trace edges of each labeled area and number each edge pixel.

Step 1-5. Select three edge pixels randomly so that the differences of the pixel numbers are all equal. Furthermore, calculate the ellipse that passes through the selected three edge pixels. Repeat this calculation 150 times and calculate the average of the center (x_{ell}, y_{ell}) , major radius r_a , minor radius r_b , and rotation angle θ_{ell} (angle of major radius and horizontal line on the camera image), respectively.

Step 1-6. Eliminate the ellipse candidates for which the

major radius r_a is smaller than 10 pixels or for which the ratio of the major radius vs. the minor radius is larger than 3.5.

Step 1-7. Calculate the average of the squared distance between the calculated ellipse in Step 1–5 and each edge pixel. Eliminate candidates for which the average is greater than 0.02.

Step 1-8. Normalize the recognized ellipses to a circle using the ratio of the major axis to the minor axis, and the rotation angle θ_{ell} of the ellipse, as depicted in Fig. 2. Set the baseline on the major radius of the recognized ellipses. The outer circle and the center circle of the marker are divided into five rings along with the radius, and each ring is divided into 20 pixels along with the arc. The middle circle is divided into 100 elements along with the arc. Each element is divided into 10 pixels along with the radius.

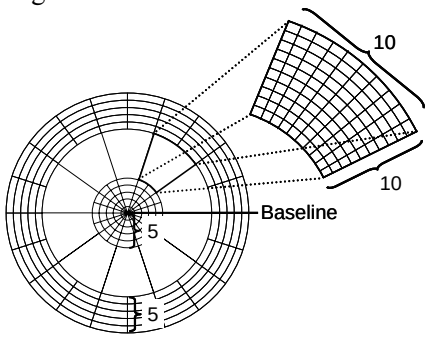

Fig. 2 Normalization of marker.

Step 1-9. Calculate the variance v_{out} and average a_{out} of pixels in the black outer circle and variance v_{in} and average a_{in} of pixels in the white center circle with the original image captured by the camera. Eliminate candidates for which v_{out} is larger than 5×10^8 or for which v_{in} is larger than 5×10^7. Set the average of a_{out} and a_{in} to a threshold th.

Step 1-10. Count pixels of each element of the middle circle divided in Step 1-8, for which the brightness is greater than th and less than th. Set the results as s_w and s_b, respectively.

Step 1-11. Find an element of the middle circle which is $s_w > s_b$ from the baseline in counterclockwise order.

Step 1-12. Find an element of the middle circle which is $s_w < s_b$ from the element found in Step 1-11 in counterclockwise order. The element found in this step is set as the basis for analyzing the binary code of the middle circle. Count the elements between the baseline and the element found in this step and set the number N_{scn}. The found element is considered as a boundary of two fans of the middle circle.

Step 1-13. Count the number of elements $s_w > s_b$ and $s_w < s_b$, respectively, from the element found in Step 1-12 in counterclockwise order for each fan. Set the results as S_w and S_b, respectively.

Step 1-14. Eliminate candidates which have a fan of $|S_w - S_b| < 3$.

Step 1-15. In all, 10 bits are obtained from the middle circle by assuming a fan for which $S_w > S_b$ is 0 and a fan for which $S_w < S_b$ is 1.

Step 1-16. Shift the 10 bits obtained in Step 1-16 10 times (circular shift in 1 bit step) and find the smallest bits. Set the result as the number of the marker. Set the number of the shift operation when the smallest bits appear as N_{sft}.

Step 1-17. Estimate four vectors $(x_{cnr}(i), y_{cnr}(i))$ (i=0,1,2,3) from the center of the marker to the four small circles using Eq. (3).

$$\begin{aligned} x_{cnr}(i) &= x\cos(\theta_{ell}) - y\sin(\theta_{ell}) \\ y_{cnr}(i) &= x\sin(\theta_{ell}) + y\cos(\theta_{ell}) \\ x &= \cos(\theta_{ell})\sin(\alpha) + \sin(\theta_{ell})\cos(\alpha) \\ y &= \{\cos(\theta_{ell})\cos(\alpha) - \sin(\theta_{ell})\sin(\alpha)\} r_b / r_a \\ \alpha &= \theta_{ell} + 3.6N_{scn} + 36N_{sft} + 45 + 90i \end{aligned} \tag{3}$$

Step 1-18. Calculate the distance l between the marker center and each ellipse recognized in Step 1-7, which is not recognized as a marker yet. Furthermore, find ellipses that are $r_b < l < 1.7r_a$.

Step 1-19. Calculate a vector v_e from the marker center to the ellipses found in Step 1-18. Find four ellipses for which the angle of v_e and $(x_{cnr}(i), y_{cnr}(i))$ is within 60 deg and the distance between the marker center and the ellipse center is shortest. The four ellipses that were found are inferred to be the four small circles of the marker.

The algorithm described above can recognize five feature points from one marker at the maximum. It is assumed that the recognition of four small circles failed and that only one feature point is obtainable from one marker if Step 1-18 or Step 1-19 has failed.

2.3 Algorithm to calculate the relative position and orientation between a camera and markers

After recognizing markers on the image, the relative position and orientation (6 degrees of freedom) between a camera and markers are estimated using the following algorithm.

Step 2-1. Select two markers so that the distance between the two markers on the image is longest if four

or more markers are recognized. Then calculate a line which passes through the two markers and select the one marker with the greatest distance from the line. Solve the P3P using the selected three markers and obtain a maximum of four possible solutions.

Step 2-2. Find markers for which four small circles are recognized if the recognized markers are fewer than four. Then solve the P3P using three small circles selected from among the four small circles and obtain a maximum of four possible solutions. The tracking fails if no marker exists for which four small circles are recognized.

Step 2-3. Estimate the position of all feature points recognized on the image using the four solutions obtained in Step 2-1 or Step 2-2, inertial parameters of the camera, and the three-dimensional position of the feature points, which were measured in advance. Then calculate the difference between the estimated position and the recognized position using the algorithm described in 2.2. That difference is called the re-projection error. Select one solution for which the re-projection error is smallest.

Step 2-4. Obtain 12 new solutions by rotating the solution by ±0.01 deg around the *x*, *y*, and *z* axes and shifting the solution by ±10 mm along the *x*, *y*, and *z* axes. Calculate the re-projection error for all new solutions. Then select the solution with the smallest re-projection error.

Step 2-5. Repeat Step 2-4 a maximum of 30 times until the re-projection error becomes less than 20 pixels.

3 Evaluation of the proposed method

To evaluate the tracking method, some experiments were conducted. The tracking method performance changes according to the radius of large circle r_1, the radius of small circle r_2, and the distance between the large circle and small circle d. However, it is difficult to evaluate the relationship between these parameters and the tracking performance in detail. In this study, therefore, one design of a multi-range marker ($d = 1.42r_1$, $r_2 = 0.12r_1$, $r_1 = 5$ cm) was evaluated. In this case, the gap separating the contour of the small circle and the large circle is equal to the outer black circle's thickness; the small circle and each fan of the middle circle are of almost equal size. The marker size becomes about 13 cm when the white area for stabilizing the recognition of the marker, which is the same size as the outer black circle's thickness, is allocated outside of the small circles.

Table 1 shows the main specifications of the hardware used for the evaluation. The software was developed using compiling software (Visual C++ 2005; Microsoft Corp. and C++ Compiler Ver.10.0; Intel Corp.) with a widely used operating system (Windows XP; Microsoft Corp.). The camera shutter speed was fixed to 10 ms; the gain was adjusted automatically during the evaluation.

Table 1 Hardware specifications used for evaluation

PC	CPU	Pentium Core2Duo 2.66 GHz
	Memory	DDR2 800 MHz, 2 GB
Camera	Vendor	Point Gray Research Inc.
	Model	Dragonfly2 XGA Black&White
	Interface	IEEE1394a
	Resolution	1024 × 768
	Frame rate	30 fps
	Focal length	8.00 mm

3.1 Maximum and minimum distance

One marker was located in front of the camera so that the camera captured the marker at the image center. The distance between the camera and marker was changed and the maximum and minimum distance at which the system can flawlessly recognize the ID of the marker 1000 times in series was evaluated. The distance at which the system can recognize the four small circles was evaluated similarly. The brightness on the marker was 700 lux. Table 2 presents the results.

Table 2 Maximum and minimum distance (mm)

Marker ID		Four small circles	
Max.	Min.	Max.	Min.
5344	251	4980	289

3.2 Stability of marker recognition under illumination change

One marker was located in front of the camera so that the camera captured the marker at the image center. The distance between the camera and marker was fixed at 1.5 m. The brightness was changed and the maximum and minimum brightness at which the system flawlessly recognized the marker ID 1000 times in series was determined. The brightness at which the system can recognize the four small circles was evaluated similarly. Table 3 represents the results. The marker can be recognized under wide illumination change.

Table 3 Maximum and minimum brightness (lux)

Step 1-1	Marker ID		Four small circles	
	Max.	Min.	Max.	Min.
Enable	3.90×10^3	6	3.88×10^3	6
Disable	3.54×10^3	12	3.46×10^3	12

3.3 Processing speed of tracking

One marker was located in front of the camera so that the camera captured the marker at the image center. The distance between the camera and the marker was fixed at about 1.5 m. We measured the time necessary for executing each process described in section 2.2 and 2.3 using the marker. Then, nine markers were placed in front of the camera on a 3×3 grid (0.5 m step vertical, 1.0 m step horizontal); the distance between the camera and the marker was fixed at about 5.0 m. We measured the necessary time for executing each process described in sections 2.2 and 2.3 using the nine markers. Table 4 presents the results. The tracking can be executed more than 60 times in a second that will be sufficient for the applications described in chapter 1.

Table 4 Necessary tracking time (ms)

Process	Required Time	
	1 marker	9 markers
Step 1-1 – Step 1-2	8.5	8.5
Step 1-3 – Step 1-4	2.9	3.4
Step 1-5 – Step 1-16	0.4	3.9
Step 1-17 – Step 1-19	0.01	Not used
Step 2-1 – Step 2-5	0.03	0.06
Total	11.9	15.9

3.4 Misrecognition of markers

To evaluate whether the algorithm described in 2.2 misrecognizes non-marker objects as markers, images captured in a water purification room of the Fugen nuclear power plant were processed using the algorithm. The images were captured by a camera held by a worker according to the scenario in which the worker walked around a water purification room checking instruments. The processed images were 19,742; among 121 images (0.61%), the algorithm misrecognized objects which were not markers as markers. Among all misrecognized cases, only the large circle was recognized; the small circles were not recognized. Figure 3 depicts two images in which the algorithm misrecognized the centers of circular valves and "0" character as markers. To avoid the misrecognition, the markers which ID is 1 and 2 should not be used for the tracking because in the 67 % of the misrecognition, non-marker object was misrecognized as these two markers, which design seems to be too simple to be used in NPPs.

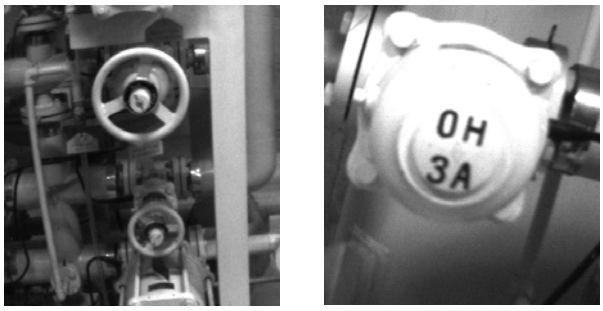

(Left) The center of the upper valve was misrecognized.
(Right) The "0" was misrecognized as a marker.

Fig. 3 Examples of misrecognized images.

3.5 Area where tracking can be executed

It is difficult to check whether the tracking can be executed at every point in a real environment if the environment is large. For this study, therefore, the area within which tracking can be executed with enough accuracy was evaluated using computer simulation. In a virtual environment, nine markers were located on a 3×3 grid (x = -1.0, 0.0, 1.0 m; y = -0.5, 0.0, 0.5 m; z = 0.0 m). The textures of nine markers were generated in 512×512 pixels including the design described in 2.1 and pasted on the virtual markers. A virtual camera for which inertial parameters (focal length, vertical and horizontal view angle and resolution) were set referring to the camera in Table 1 was moved in 1 cm steps in an area ($-3.0 \le x \le 3.0$ m; $-0.5 \le y \le 0.5$ m; $0.0 \le z \le 6.0$ m) in front of the markers. The camera direction was fixed to -z direction. We then checked whether tracking can be executed at every point by generating the camera image using OpenGL library and applying the algorithm described in 2.2 and 2.3 (Total 601×101×601 = 36,481,301 points). Figure 4 shows an image generated using OpenGL library. In this image, imperfection of the distortion correction and focal depth of the camera were not accurately simulated, but we can roughly estimate the area within which the tracking can be executed.

Fig. 5 shows the points at which the position and orientation error of the tracking is less than 20 cm and 20 deg respectively when the camera was moved on a plane (y = 0). If the distance between the marker and the camera is greater than about 3 m, the accuracy and stability of the tracking is not enough if the camera can capture less than four markers. If the distance is greater

than about 5 m, the accuracy and stability is not enough even if the camera can capture not less than four markers. This means that the tracking with the small circles are effective at less than 3 m and the tracking with the large circle is effective at less than 5 m. The number of points at which the algorithm used not less than four markers at between 3 m and 5 m, and at shorter than 5 m were, respectively, a = 4,269,416 and b = 4,898,851. The number of points at which the tracking can be executed with single marker at shorter than 3 m was c = 5,635,046. Therefore, the area within which the tracking can be executed using multi-range markers is (c-b+a)/a×100 = 117.2 % and a/c×100 = 75.8 % larger than that of the circle marker and the square marker respectively.

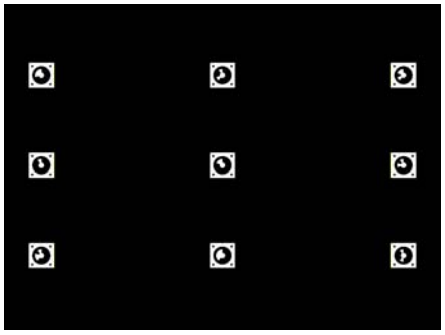

Fig. 4 Example of an image generated using OpenGL.

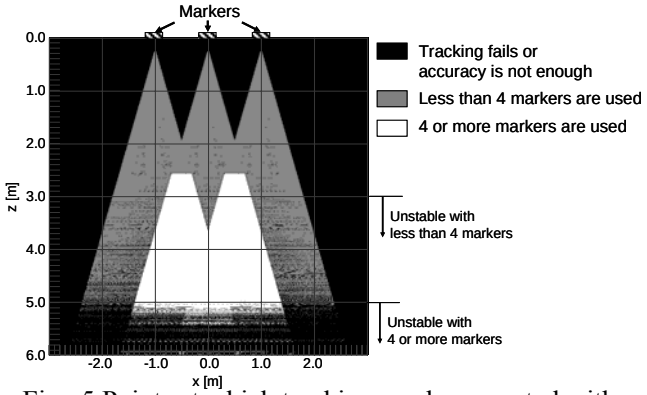

Fig. 5 Points at which tracking can be executed with enough accuracy (Top view of the area).

4 Conclusions

For this study, a new marker that is useful for both long and short distances was designed. An algorithm for recognizing the markers and using them for augmented reality tracking was also developed. Results of evaluation experiments demonstrate that the new marker can increase the area for tracking compared to that for circular and square markers. Moreover, the algorithm can recognize markers under severe environmental conditions, with very high and very low brightness, and where the distance between a camera and the markers is great. Future studies will evaluate the feasibility of the proposed markers and the algorithm in an actual nuclear power generation environment.

References

[1] R. Azuma, et al. Recent Advances in Augmented Reality [J]. IEEE Computer Graphics and Applications, 2001, 21(6): 34-47.

[2] H. Shimoda, et al. A Support System for Water System Isolation Task of Nuclear Power Plant by using Augmented Reality and RFID [J], Maintenology, 2004, 3(2): 30-37.

[3] H. Ishii, et al. Proposal and Evaluation of Decommissioning Support Method of Nuclear Power Plants using Augmented Reality [J]. Transactions of the Virtual Reality Society of Japan, 2008, 13(2). (In press)

[4] N. Navab. Developing Killer Apps for Industrial Augmented Reality [J]. IEEE Computer Graphics and Applications, 2004, 24(3): 16-20.

[5] H. Kato, et al. Marker Tracking and HMD Calibration for a Video-based Augmented Reality Conferencing System [A]. Proceedings of International Workshop on Augmented Reality [C]. San Francisco: IEEE and ACM, 1999, 85-94.

[6] M. Appel, et al. Registration of technical drawings and calibrated images for industrial augmented reality [A]. Proceedings of IEEE Workshop on Applications of Computer Vision [C]. California:IEEE, 2000, 48-55.

[7] X. Zhang, et al. Taking AR into large scale industrial environments: Navigation and information access with mobile computers [A]. Proceedings of IEEE International Symposium on Augmented Reality [C]. New York:IEEE, 2001, 179-180.

[8] Z. Bian, et al. Development of a Tracking Method for Augmented Reality Applied to NPP Maintenance Work and its Experimental Evaluation [J], IEICE TRANSACTIONS on Information and Systems, 2007, E90-D(6): 963-974.

[9] H. Ishii, et al. Development and Evaluation of Tracking Method for Augmented Reality System for Nuclear Power Plant Maintenance Support [J], Maintenology, 2007, 5(4): 59-68.

[10] L. Naimark, et al. Circular Data Matrix Fiducial System and Robust Image Processing for a Wearable Vision-inertial Self-tracker [A]. Proceedings of International Symposium on Mixed and Augmented Reality [C], Darmstadt:IEEE, 2002, 27-36.

[11] L. Quan, et al. Linear N-Point Camera Pose Determination [J], IEEE Transactions on Pattern Analysis and Machine Intelligence, 1999, 21(7):774-780.

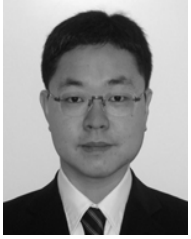

ISHII Hirotake was born in 1973. He is an assistant professor of Kyoto University. His current research interests include augmented and virtual reality, human-computer interaction.